Effects of Self-Consistent Flow on Island Generation in Interchange Mode

J. Plasma Fusion Res. SERIES, Vol. 6 (2004) 589–592

Effects of Self-Consistent Flow on Island Generation in Interchange Mode

ICHIGUCHI Katsuji and CARRERAS Benjamin A.[1]
National Institute for Fusion Science, Toki 509-5292, Japan
[1]Oak Ridge National Laboratory, Oak Ridge, Tennessee 37831, USA
(Received: 9 December 2003 / Accepted: 23 April 2004)

Abstract

The time evolution of magnetic island in the nonlinear phase of the resistive interchange mode is examined in the cylindrical geometry. The effects of self-consistent uniform poloidal flow is taken into account. In this case, the reconnection of the magnetic field line occurs both at the saturation of the dominant unstable mode and at the saturation of the $n = 0$ mode, where n is the toroidal mode number, through the curvature change of perturbed poloidal flux surface.

Keywords:

magnetohydrodynamics (MHD), resistive interchange mode, magnetic island, driven reconnection

1. Introduction

The interchange mode is a dangerous magnetohydrodynamic (MHD) instability in zero-current stellarators. In the linear analysis, the eigenfunction for the poloidal magnetic flux corresponding to the maximum growth rate is an odd function in the radial coordinate. Therefore, the flux is close to zero at the resonant surface even with finite resistivity. This means that magnetic islands are hardly generated spontaneously in the linear phase, not like the tearing mode. On the other hand, the numerical study for the Large Helical Device (LHD) plasma in the toroidal geometry showed that the magnetic islands can be generated in the nonlinear saturation phase of the interchange mode evolution [1]. The number of the island on a poloidal cross section is twice of the poloidal mode number of the driving interchange mode. Similar islands were obtained in the nonlinear calculations for Heliotron E plasmas [2,3]. Thus, we consider the mechanism of the island generation in the nonlinear saturation of the interchange mode. In the present study, we also take the effect of the self-consistent poloidal uniform flow into account by including both parity of sine and cosine in the Fourier expansion for each perturbation.

2. Basic equations and configurations

We study the island generation by using the NORM code [1]. This code solves the nonlinear reduced MHD equations for poloidal magnetic flux ψ, stream function Φ and plasma pressure P. In order to examine the generation mechanism of the magnetic island precisely, we study the nonlinear saturation of the interchange mode in the cylindrical geometry (r, θ, z). In this case, the reduced equations are expressed as $\frac{\partial \psi}{\partial t} = -\boldsymbol{B}\cdot\nabla\Phi + \frac{1}{S} J_z$, $\frac{dU}{dt} = -\boldsymbol{B}\cdot\nabla J_z + \frac{\beta_0}{2\varepsilon^2} \nabla\Omega \times \nabla P\cdot\boldsymbol{e}_z + \nu\nabla_\perp^2 U$, and $\frac{dP}{dt} = \kappa_\perp \nabla_\perp^2 P$. The convective time derivative is given by $\frac{d}{dt} = \frac{\partial}{\partial t} + \boldsymbol{v}_\perp\cdot\nabla$ where $\boldsymbol{v}_\perp = \nabla\Phi \times \boldsymbol{e}_z$. The magnetic field $\boldsymbol{B}$ is given by $\boldsymbol{B} = B_0\boldsymbol{e}_z + \boldsymbol{e}_z \times \nabla\psi$, where $\boldsymbol{e}_z$ means the unit vector in z direction. The subscripts of '0' and '$\perp$' mean the value at the magnetic axis and the vector component perpendicular to z direction, respectively. The factor of $\varepsilon \equiv a/R_0$ is the ratio of the minor and the major radii of the corresponding torus, and β_0 denotes the beta value at the axis. The time is normalized by the poloidal Alfvén time, τ_A. The vorticity U and the toroidal current density J_z are given by $U = \nabla_\perp^2\Phi$ and $J_z = \nabla_\perp^2\psi$, respectively. The vector of $\nabla\Omega$ denotes the average curvature of the field line which drives the interchange mode with the pressure. The perturbation $\widetilde{X}(r, \theta, z)$ are expanded in the Fourier series in the way of $\widetilde{X} = \sum_{mn}\widetilde{X}^c_{mn}(r) \cos(m\theta - n\zeta) + \sum_{mn}\widetilde{X}^s_{mn}(r) \sin(m\theta - n\zeta)$, where X denotes ψ, Φ or P and $\zeta = z/R_0$. The component of $\widetilde{\Phi}^c_{00}$ corresponds to the poloidal uniform flow.

In the present study, we employ a straight equilibrium corresponding to the LHD configuration with the vacuum magnetic axis located at $R_{ax} = 3.6$m [1]. The equilibrium is calculated with no net current and the pressure profile of $P = P_0(1 - r^4)^2$ with $\beta_0 = 2\%$. In this equilibrium, the rational surface with $\iota = 1/2$ is included in the plasma column. Thus, we consider the single helicity perturbation with $m/n = 2/1$. The modes of $0 \le n \le 7$ and 768 radial grids are used in the numerical calculation. In the nonlinear calculation, we employ a fairly large magnetic Reynolds number, $S = 10^4$, so

Corresponding author's e-mail: ichiguch@nifs.ac.jp

as to make the feature of the magnetic island prominent. We also choose the fluid viscosity of $\nu = 10^{-3}$ and perpendicular heat conductivity $\kappa_\perp = 10^{-4}$ so that the $(m, n) = (2, 1)$ component should have the largest linear growth rate.

3. Time evolution of island structure

Figure 1 shows the time evolution of the kinetic energy of the perturbation, which is defined by $E_k = \sum_n E_k^n$, $E_k^n = \frac{1}{2}\int [|\nabla_\perp \sum_m \tilde{\Phi}^c_{mn} \cos(m\theta - n\zeta)|^2] + |\nabla_\perp \sum_m \tilde{\Phi}^s_{mn} \sin(m\theta - n\zeta)|^2] \mathrm{d}V$. The dominant mode is $(m, n) = (2, 1)$ mode in the whole time evolution. All of the components with $n \geq 1$ saturate at $t = 3{,}500\tau_A$, while the $n = 0$ mode grows quite slowly and saturates around $t = 17{,}000\tau_A$.

Figure 2 shows the flow pattern on the poloidal cross section at $z = 0$. We also plot the position of the resonant surface where the total rotational transform ι_T equals to 1/2, which is defined by $\iota_T(r, \theta, z) = \frac{1}{r}\frac{\partial}{\partial r}[\psi_{eq}(r) + \tilde{\psi}(r, \theta, z)]\frac{R_0}{B_0}$, as well as the position of $\iota_{eq} = 1/2$. Here the tilde and the subscript of '*eq*' mean the perturbed and the equilibrium quantities, respectively. In Fig. 2(a), four vortices are seen around the resonant surface. This pattern corresponds to the typical linear eigenfunction of the interchange mode with $m = 2$. The surface with $\iota_T = 1/2$ is deformed mainly by the radial component of the flow at the dominant mode saturation. This flow pattern is almost kept until the $n = 0$ components becomes comparable with the dominant mode. As the $n = 0$ component grows, the flow pattern varies. At $t = 18{,}000\tau_A$, the uniform poloidal shear flow is seen particularly inside the resonant surface in Fig. 2(b).

Since we treat the single helicity perturbation, the structure of the magnetic island can be observed by plotting the helical magnetic flux ψ_h, which is defined by $\psi_h(r, \theta, z) = \tilde{\psi}(r, \theta, z) + \psi_{eq}(r) - \psi_{mn}(r)$, $\psi_{mn}(r) = \frac{1}{2} r^2 \frac{n}{m}\frac{B_0}{R_0}$. Figure 3 shows the contour of the helical flux on the poloidal cross section at $t = 3{,}000\tau_A$, $9{,}600\tau_A$ and $t = 18{,}000\tau_A$. At $t =$

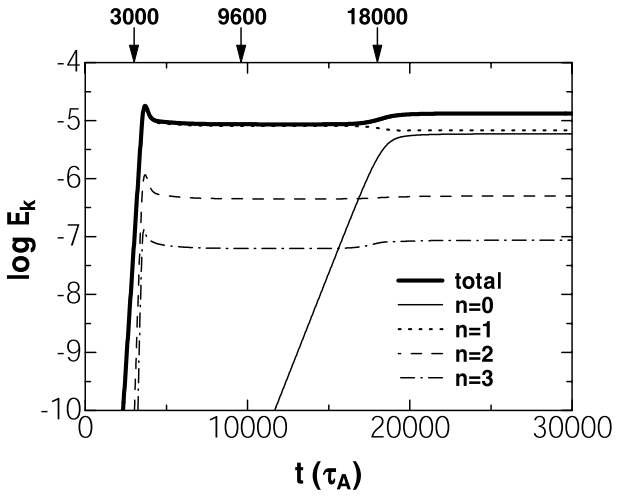

Fig. 1 Time Evolution of the kinetic energy.

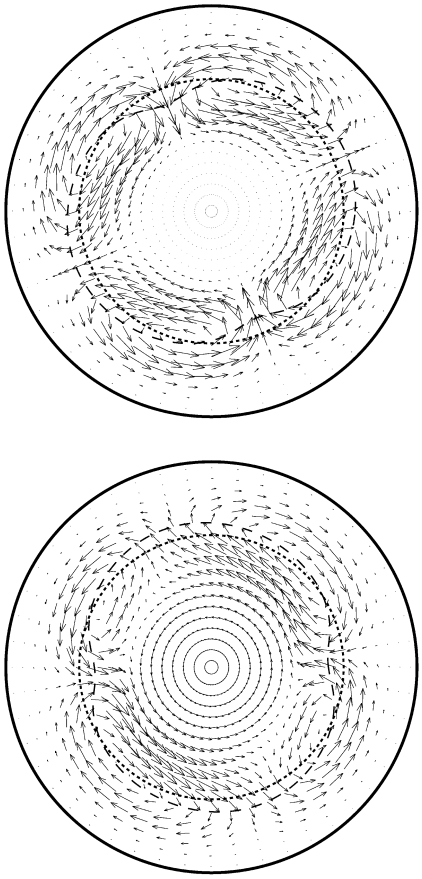

Fig. 2 Flow pattern at (a) $t = 9{,}600\tau_A$ and (b) $t = 18{,}000\tau_A$ for $r \leq 0.8$. Dotted and dashed lines show the position of the surfaces with $\iota_T = 1/2$ and $\iota_{eq} = 1/2$, respectively.

$3{,}000\tau_A$ in the linear phase, two thin islands are observed, as shown in Fig. 3(a). The island structure is consistent with the linear eigenfunction of the resistive interchange mode for the large resistivity. Therefore, these islands are considered to be generated spontaneously. The X-points of the spontaneous islands are maintained through the whole time evolution. We call them major X-points here.

At the saturation of the dominant mode, the reconnection of the field line occurs and new X-points are generated at the positions of the O-points of the spontaneous islands, as shown in Fig. 3(b). These X-points are called minor X-points. The number of the island is increased to four. As shown in Fig. 3(c), the minor X-points are annihilated when the $n = 0$ mode is saturated. The number of the island is reduced to two. The shape of the resultant island is asymmetry with respect to the O-point and the whole island structure is rotated in the poloidal direction.

4. Mechanism of reconnection

The generation and the annihilation of the minor X-points are related to the radial component of the perturbed magnetic field, B_r. Figure 4 shows the profile of B_r along the resonant surface in the poloidal cross section. The zero points at $\theta = 0.13\pi$ and 1.13π correspond to the O-points at $t = 3{,}000\tau_A$, while they correspond to the minor X-points at $t =$

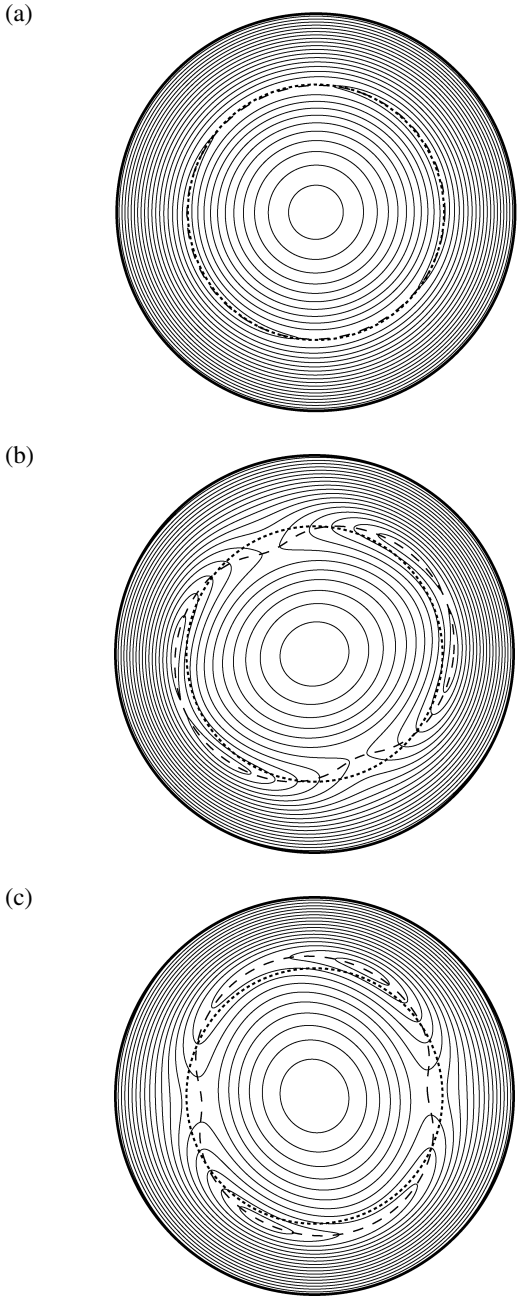

Fig. 3 Contour of ψ_h at (a) $t = 3{,}000\tau_A$, (b) $t = 9{,}600\tau_A$ and (c) $t = 18{,}000\tau_A$ for $r \leq 0.8$. Dotted and dashed lines show the position of the surfaces with $\iota_T = 1/2$ and $\iota_{eq} = 1/2$, respectively.

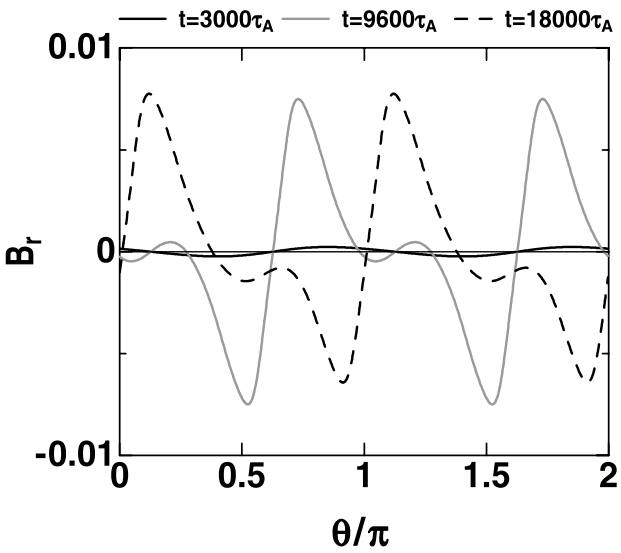

Fig. 4 Plots of B_r along the resonant surface.

$9{,}600\tau_A$. At $\theta = 0.2\pi$ and 1.2π in the vicinity of the minor X-points, B_r is negative at $t = 3{,}000\tau_A$ while it is positive at $t = 9{,}600\tau_A$. At $t = 18{,}000\tau_A$, B_r becomes negative again at $\theta = 0.66\pi$ and $\theta = 1.66\pi$ in the vicinity of the positions of $\theta = 0.5\pi$ and $\theta = 1.5\pi$ where the minor X-points are annihilated. Therefore, the direction of B_r reverses in the generation and the annihilation of the minor X-points.

The change of the sign of B_r can be explained with the geometrical structure of the perturbed poloidal flux surface because the perturbed magnetic field is tangential to the $\tilde{\psi}$ contour. Figure 5 shows the schematic picture of the contour of $\tilde{\psi}$ in the poloidal cross section. The horizontal direction corresponds to $\theta = 0.13\pi$ in Fig. 5(a) and (b) and to $\theta = 0.5\pi$ in Fig. 5(c). The surfaces of $\tilde{\psi} = const.$, $r = const.$ and $\iota_T = 1/2$ are plotted which cross at $\theta = 0.2\pi$ for $t = 3{,}000\tau_A$ and $t = 9{,}600\tau_A$ and at $\theta = 0.66\pi$ for $t = 18{,}000\tau_A$. At $t = 3{,}000\tau_A$, the radial curvature of the $\tilde{\psi} = const.$ surface is smaller than $1/r$. This means that B_r is negative at $\theta = 0.2\pi$. At $t = 9{,}600\tau_A$, as shown in Fig. 5(b), the radial curvature of the $\tilde{\psi} = const.$ surface is larger than $1/r$ at the same position. This means that B_r is positive. The enhancement of the curvature is attributed to the outward flow of the vortex which is shown in Fig. 2(a).

When the $n = 0$ mode becomes comparable to the $n = 1$ mode, the position of the maximum outward velocity deviates from the minor X-point in the poloidal direction. At $t = 18{,}000\tau_A$, the maximum outward velocity position is located at $\theta = 0.66\pi$ as shown in Fig. 2(b), while the position of the original minor X-points corresponds to $\theta = 0.5\pi$. Therefore, the $\tilde{\psi} = const.$ surface around $\theta = 0.66\pi$ is pushed out by the flow. On the other hand, the effect of the outward flow is small around $\theta = 0.33\pi$. As a result, the structure of the $\tilde{\psi} = const.$ surface becomes asymmetry with respect to the minor X-point as shown in Fig. 5(c). The curvature of the $\tilde{\psi} = const.$ surface is decreased only for $\theta \geq 0.5\pi$ to the value less than $1/r$. Then, the direction of B_r reverses and the island disappears at only one side of the minor X-point. The resultant island has asymmetric structure with respect to the O-point as shown in Fig. 3(c).

5. Conclusions

The magnetic islands can be generated and annihilated in the nonlinear saturation of the interchange mode.

In the saturation of the dominant unstable mode, the radial flow due to the vortex can change the O-point to the minor X-point. Then, the original island is divided into two islands. In this case, the curvature enhancement of the perturbed flux surface is essential in the minor X-point generation. This mechanism is different from the standard driven

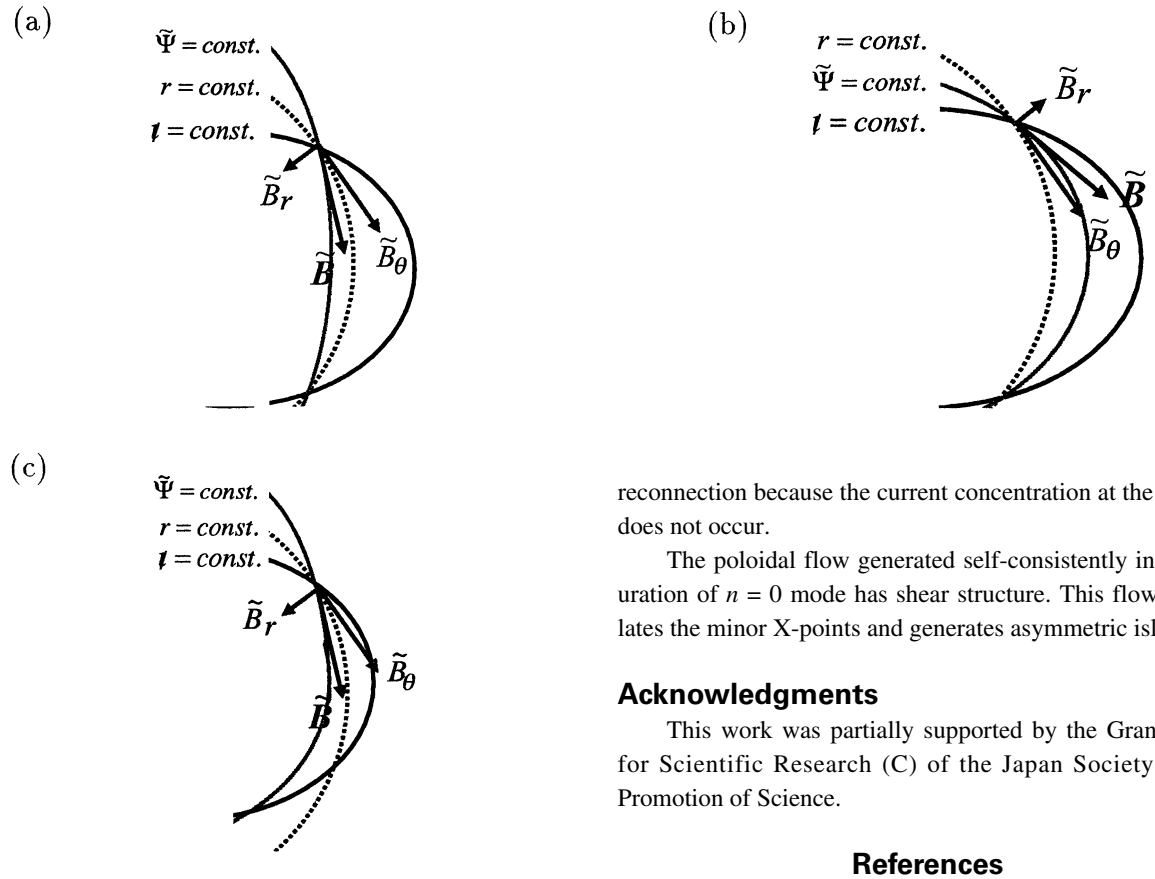

Fig. 5 Schematic pictures of $\tilde{\psi}$ at (a) t = 3,000τ_A, (b) t = 9,600τ_A and (c) t = 18,000τ_A.

reconnection because the current concentration at the X-point does not occur.

The poloidal flow generated self-consistently in the saturation of n = 0 mode has shear structure. This flow annihilates the minor X-points and generates asymmetric islands.

Acknowledgments

This work was partially supported by the Grant-in-Aid for Scientific Research (C) of the Japan Society for the Promotion of Science.

References

[1] K. Ichiguchi *et al.*, Nucl. Fusion **43**, 1101(2003).
[2] M. Wakatani *et al.*, Nucl. Fusion **24**, 1407 (1984).
[3] B.A. Carreras *et al.*, Phys. Plasmas **10**, 3700 (1998).